

Development of Low-Noise / Low-Power Preamplifier for the Readout of Inorganic Scintillators and their Mass Production Test System

This content has been downloaded from IOPscience. Please scroll down to see the full text.

2015 J. Phys.: Conf. Ser. 587 012024

(<http://iopscience.iop.org/1742-6596/587/1/012024>)

View [the table of contents for this issue](#), or go to the [journal homepage](#) for more

Download details:

IP Address: 131.152.112.139

This content was downloaded on 13/03/2017 at 10:37

Please note that [terms and conditions apply](#).

You may also be interested in:

[Low-Power and High-Speed Technique for logic Gates in 20nm Double-Gate FinFET Technology](#)

A Priydarshi and M K Chattopadhyay

[Low-Power and High-Sensitivity Magnetoresistive Random Access Memory Sensing Scheme with Body-Biased Preamplifier](#)

Takeaki Sugimura, Jun Deguchi, Hoon Choi et al.

[AN INTEGRATING PREAMPLIFIER FOR INDIUM ANTIMONIDE INFRARED DETECTORS](#)

J. R. Barton and D. A. Allen

[A low-noise widely tunable Gm-C filter with frequency calibration](#)

Wang Yu, Liu Jing, Yan Na et al.

[Reactive ion etching of silicon using low-power plasma etcher](#)

D S Veselov, A D Bakun and Yu A Voronov

[Two-phase low-power analogue CMOS peak detector with high dynamic range](#)

E Malankin

[Multi-mode multi-band power amplifier module with high low-power efficiency](#)

Zhang Xuguang and Jin Jie

[Development of ATLAS Liquid Argon Calorimeter front-end electronics for the HL-LHC](#)

T. Liu

[Design and performances of a low-noise and radiation-hardened readout ASIC for CdZnTe detectors](#)

Gan Bo, Wei Tingcun, Gao Wu et al.

Development of Low-Noise / Low-Power Preamplifier for the Readout of Inorganic Scintillators and their Mass Production Test System

I. Keshelashvili, W. Erni, F. Müller, M. Steinacher, B. Krusche

Department of Physics, University of Basel, Klingelbergstrasse 82, CH-4056 Basel, Switzerland

E-mail: i.keshelashvili@unibas.ch

Abstract. The development of the preamplifier and all test procedures done by our group during the past several years at the University of Basel will be discussed. In addition, we present the results from the testing of the first 1'500 channels of the preamplifiers for the Crystal Barrel experiment using a specially developed automatized test system.

1. Introduction

Photomultiplier tubes like vacuum-photo-tetrode (VPTT) and semiconductor photosensors like avalanche photodiode (APD) have the important advantage over multi-dynode photomultipliers (PMT's) that they can be operated in reasonably strong magnetic fields. They have, however, much lower gains than PMT's, which requires well adapted preamplifiers. We have developed, the so called Basel-LNP (Low-Noise / Low-Power) preamplifier, which is a very sensitive charge to voltage converter/amplifier. The basic concept is a discrete element design preamplifier (that can be easily adapted to different requirements) for the first stage of the readout of low amplification photosensors. Two version of the LNP have been optimized for the readout of the forward end-cap of the electromagnetic calorimeter of the PANDA detector, which is under design for the planned FAIR facility. One will be used for the inner sections equipped with VPTT's, the other for the outer sections equipped with APD's. For this detector a very high dynamic range ($\sim 10^4$) and high count-rates (max. 1 MHz) are expected. In addition, crystals and preamplifiers have to be operated at temperatures of -25°C , which strictly limits the acceptable energy dissipation of the LNP. Another version of the LNP has been optimized for an upgrade of the Crystal Barrel detector at the ELSA accelerator (Bonn) which consists of CsI(Tl) crystals. The upgrade from the current readout of the scintillators by photodiodes to APD's will provide so far missing timing information from the scintillators (particularly important for triggering). A special feature of this system is the compensation of gain changes of the APD's due to temperature variations by a feed-back of the temperature information on their HV supplies.

1.1. The Crystal Barrel detector

The Crystal Barrel detector [1, 2] is a large acceptance electromagnetic calorimeter designed to measure charged and neutral particles up to a few GeV. The current setup counts 1'230 CsI(Tl)



crystals. Each crystal is $16.1 X_0$ radiation length thick and covers $6^\circ \times 6^\circ$ degree in polar and azimuthal angle between 30° – 150° and $12^\circ \times 6^\circ$ between 150° – 156° (only 30 crystals). In the past, it was designed to operate inside a strong solenoid magnet at the LEAR (Low Energy Antiproton Ring) ring at CERN. Due to the presence of a strong magnetic field, the readout of the crystals used PIN diodes. This has the large disadvantage that no timing information is provided. Now, at the Electron Stretcher Accelerator ELSA at the University of Bonn the device is no longer operated in magnetic fields and mainly used for measurements of final states with high photon multiplicity. Ideally, one would like to trigger on the photons, but since the detector provides no timing information most triggers have to rely on signals from charged particles in a cylindrical scintillating fiber detector surrounding the target. This is in particular a problem for reactions off quasi-free neutrons, where no recoil proton can provide the trigger. Therefore it will be equipped with large area ($\sim 1\text{cm}^2$) avalanche photodiodes [3]. Each crystal of the detector will be read out by two APD's of the type Hamamatsu S11048(X3). The dual channel, single board Basel-LNP preamplifier will be the first stage in the front-end electronics (FEE) followed by a signal shaper and the readout electronics.

1.2. The PANDA detector

The PANDA detector will be one of the major detectors of the FAIR facility at the GSI Darmstadt. It is planned as a high luminosity, internal experiment operating with intense antiproton beams on a fixed target at the HESR (High Energy Storage Ring). Basically all branches of the planned experimental program [4] require an electromagnetic calorimeter [5] with excellent energy, position, and time resolution. In order to meet this requirement, the PANDA EM calorimeter will have more than 15'000 PWO crystals of 22 radiation lengths X_0 and with a front face of $\sim 2 \times 2$ cm. In contrast to the PWO crystals used in the CMS experiment at CERN, the PANDA experiment will be equipped with second generation scintillators from the recently developed material which roughly doubles the light output. Furthermore, the whole PANDA EMC will be cooled down to -25° degree Celsius because at this temperature the number of photons emitted by PWO is three times higher than at room temperature. The PWO crystals in the electromagnetic calorimeter will be distributed in three main groups: forward end-cap having 3'856 crystals, central barrel having 11'360, and backward end-cap having 528 crystals. The PANDA EMC will be placed inside the 2 T solenoid magnet which excludes the use of conventional multistage PMT's. Therefore the crystals will be read out by specially developed Hamamatsu Large Area Avalanche Photodiodes (LAAPD, tow sensors per crystal). Only in the extreme forward direction close to the beam the crystals will be equipped with Vacuum-Photo-Tetrodes (VPTT, Hamamatsu R11375-01), in order to guarantee radiation hardness and to cope with the high count rates. The two types of preamplifiers designed in Basel for this end-cap will be the only active electronic devices located inside the cold area.

2. Preamplifier

The design of the preamplifiers for the Crystal Barrel detectors allows amplification of two separate APD signals (each scintillator is read out by two APD's) with two electrically identical channels placed onto one Printed Circuit Board (PCB). The electronic circuit of a single channel is shown in Fig.: 1. The Basel-LNP preamplifier is an operational amplifier with a field-effect transistor JFET at its input with the feed-back capacitance C12 (6.8pF). At the input, we have first the decoupling capacitor C1 (4.7nF) followed by low-noise protection diodes D1 and D2. The output rise time (~ 40 ns) and the noise level is mainly set by the JFET, while the R11+R12 direct feed-back resistors determine the signal fall-time constant ($\sim 60\mu\text{s}$). This preamplifier is powered by +8 V and -2 V, dissipating 12 mA and 6 mA current respectively. The maximum current with 10 kHz count-rate and at the maximum amplitude is ~ 18 mA (+8 V) and ~ 9 mA (-2 V).

for current leakage. The main focus in this test is to check the ceramic capacitors and resistors of the bias voltage for possible damages. The second test involves measurements with several different amplitudes and different hit rates. The raw information from a sampling ADC is saved into output files, which allows the analysis of the line shape of the signal, its time characteristics and amplitude linearity. It is also monitored that the noise level is within acceptable limits. The test procedure is generated by a Linux based computer system controlling the four main components, which are shown in Fig.: 3. The first device (starting from the left hand side), is

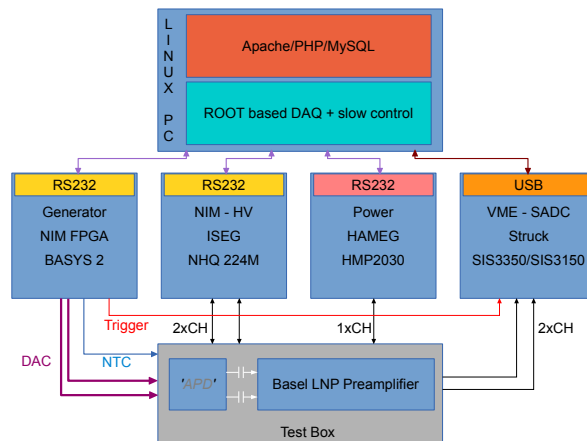


Figure 3. Setup of the test system with its main components.

a custom-built, single-width NIM module which combines a standard Digilent Basys 2 FPGA board with two standard and two custom made peripheral modules (Pmod) shown in Fig.: 4. The standard Pmods are a RS232 serial-converter interface and a 16 bit digital-to-analog (DAC) converter. They define the reference level for the output voltage generator, which uses Schmitt triggers (shown in Fig.: 4). The fourth custom peripheral module generates the TTL trigger signal for the flash ADC. The high voltage test (second module from the left), uses a dual channel, high

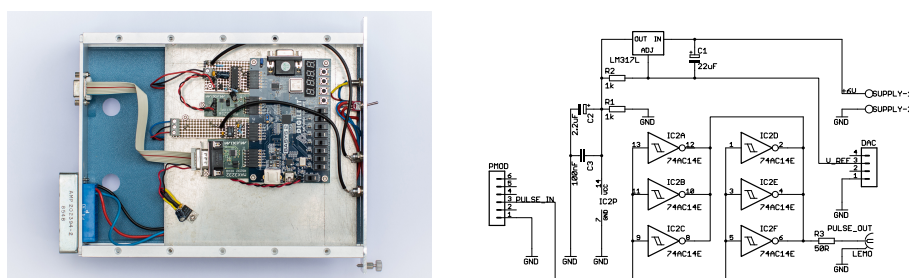


Figure 4. Left: Custom made NIM-FPGA based pulse generator module. Right: Schematic of the output driver.

precision ISEG NHQ 224M module (single width NIM standard), which is RS232 compatible and capable to measure voltage and current with 1 nA resolution [7]. For the monitoring of the power consumption during the test, the programmable power supply HAMEG HMP2030 has been used [8]. It is also RS232 compatible and is monitoring the voltage (+8 V and -2 V) and the corresponding current consumption. The third channel of the power supply has been used as a relay to switch from the high voltage test to the amplitude or signal testing mode.

It was especially electrically separated, in order to avoid any possible damage of the amplifier. The fourth and last module is the VME readout system capable to digitize all input and output signal shapes using a 500MS/s flash ADC from Struck [10]. The readout of the VME bus was done with a high performance USB to VME interface [9].

The signal generated by the FPGA pulsed generator (shown left on Fig.: 2) is passively split (R1, R2, R3 resistors) inside the test box (Fig.: 5) to simulate charge bursts (C1, C2 capacitors, generate charge out of voltage) of the photo sensor. The capacitors C3 and C4 on the right hand side of Fig.: 5 are equivalent to the capacitance of the APD under bias voltage. The

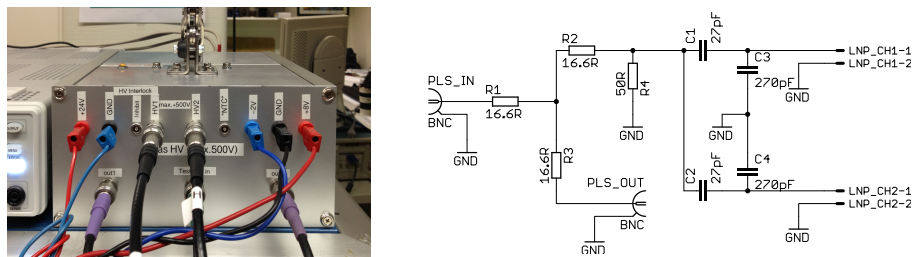


Figure 5. The test box for the Crystal Barrel preamplifiers.

software controlling the test system has a modular architecture and is based on the CERN ROOT package [11]. It has a graphical interface and can be easily customized to select the optimal test procedure.

4. Results

So far, we have tested 756 dual channel preamplifiers, which is effectively more than 1500 separate channels of the Crystal Barrel type preamplifier. Out of them, we have rejected only about 2.5% due to different failures. This results were much below of the expected rejection rate. Less than 1% of the preamplifiers were electrically damaged, probably due to malfunctioning of some electric components. The rest was rejected due to the so-called tombstone effect caused by a special soldering procedure which, in fact, created this problem for the surface mountable device (SMD) components, shown in Fig.: 6. As a first step, the components of the bias voltage

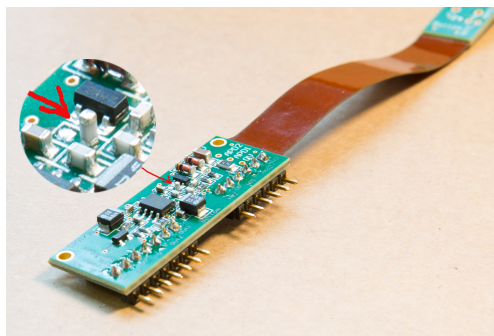


Figure 6. The rejected Crystal Barrel type preamplifier due to the tombstone effect (this is an SMD component that is partially or completely lifted off one end of the soldering pad).

are tested for their absolute maximum voltage of +500V (that will never be the case in the real experiment). In this test, we simply secure the normal operation of the resistors and the ceramic capacitors. The whole HV test takes about 30 sec with 100V/sec ramping time. During this test, the voltage stability test and the current leakage is monitored, see left hand side of

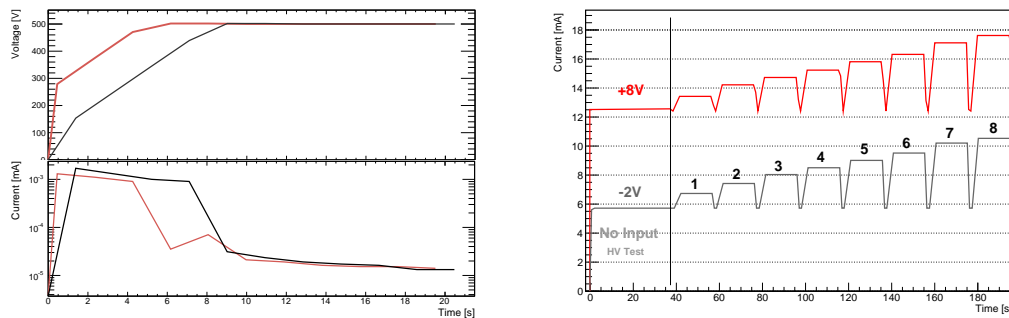


Figure 7. Left hand side: High voltage test, top the voltage and bottom the current vs time. Right hand side: Current consumption of the preamplifier during the test.

Fig.: 7. The right hand side of the same picture shows the current consumption during the whole test. The first ~ 40 seconds shows the minimal power consumption (without input signal) of the preamplifier. After the HV test, the power consumption of eight different amplitudes, evenly distributed over the whole dynamic range of the output, is measured with the maximum expected count-rate of 10 kHz. The gain of each channel is extracted by linear fitting of the eight different

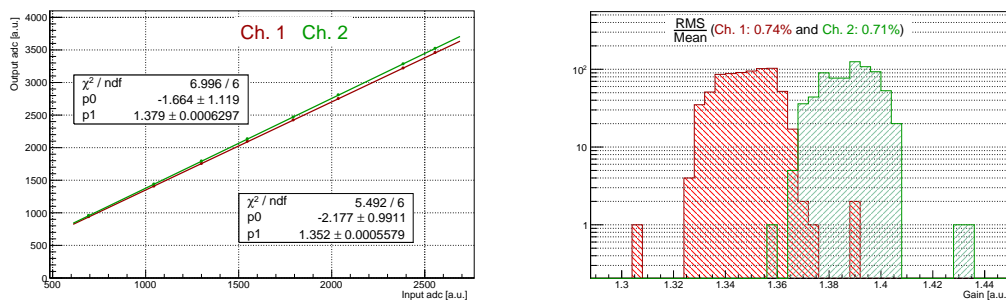


Figure 8. Left hand side: The graph of an output voltage dependence vs. input voltage and Right hand side: The gain distribution of the first (red) and second (green) channels is shown.

amplitudes. It is shown at the lefthand side of Fig.: 8. The slope (gain) and the amplitude linearity is extracted for each preamplifier channel and is stored into the database (together with other important parameters) for a quick overview and the selection of the best preamplifier modules for the experiment. The right hand side of Fig.: 8 shows $\sim 0.7\%$ (RMS/Mean) spread of the gain distribution, which is significantly lower than the light output differences between different crystals.

References

- [1] E. Aker et al. 1992 NIM A321 69.
- [2] G. Suft et al. 2005 NIM A538 416
- [3] Christoph Wendel (for the CBELSA/TAPS Collaboration) 2009 J. Phys.: Conf. Ser. 160 012006
- [4] Physics Book - PANDA http://www-panda.gsi.de/archive/public/panda_pb.pdf
- [5] Technical Design Report - PANDA EMC http://www-panda.gsi.de/archive/public/panda_tdr EMC.pdf
- [6] BasysTM2 Spartan-3E FPGA Board <http://www.digilentinc.com/BASYS2>
- [7] ISEG NHQ 224M <http://www.iseg-hv.com/en/products/product-details/product/15/>
- [8] HAMEG HMP2030 <http://www.hameg.com/0.723.0.html>
- [9] SIS3150-USB USB2.0 to VME interface <http://www.struck.de/sis3150usb.htm>
- [10] SIS3350 4 Channel 500 MS/s 12-bit ADC/Digitizer <http://www.struck.de/sis3350.htm>
- [11] CERN ROOT library <http://root.cern.ch>